The peroxisome proliferator-activated receptor-γ agonist troglitazone inhibits transforming growth factor-β–mediated glioma cell migration and brain invasion

Roland Coras,[1] Annett Hölsken,[1] Sebastian Seufert,[4] Jan Hauke,[4] Ilker Y. Eyüpoglu,[2] Martin Reichel,[3] Christian Tränkle,[5] Florian A. Siebzehnrübl,[1] Rolf Buslei,[1] Ingmar Blümcke,[1] and Eric Hahnen[1,4]

Departments of [1]Neuropathology, [2]Neurosurgery, and [3]Experimental Medicine II, University of Erlangen, Erlangen, Germany; [4]Institute of Human Genetics, Institute of Genetics, and Center for Molecular Medicine Cologne, University of Cologne, Cologne, Germany; and [5]Department of Pharmacology and Toxicology, Institute of Pharmacy, University of Bonn, Bonn, Germany

Abstract

Gliomas are the most common primary tumors of the central nervous system, with glioblastomas as the most malignant entity. Rapid proliferation and diffuse brain invasion of these tumors are likely to determine the unfavorable prognosis. Considering its promigratory properties, the transforming growth factor-β (TGF-β) signaling pathway has become a major therapeutic target. Analyses of resected glioma tissues revealed an intriguing correlation between tumor grade and the expression of TGF-$\beta_{1\text{-}3}$ as well as their receptors I and II. Here, we analyzed the effects of peroxisome proliferator-activated receptor γ (PPAR-γ) agonists on glioma proliferation, migration, and brain invasion. Using an organotypic glioma invasion model, we show that micromolar doses of the PPAR-γ activator troglitazone blocked glioma progression without neurotoxic damage to the organotypic neuronal environment observed. This intriguing antiglioma property of troglitazone seems to be only partially based on its moderate cytostatic effects. We identified troglitazone as a potent inhibitor of glioma cell migration and brain invasion, which occurred in a PPAR-γ–independent manner. The antimigratory property of troglitazone was in concordance with the transcriptional repression of TGF-$\beta_{1\text{-}3}$ and their receptors I and II and associated with reduced TGF-β release. Due to its capacity to counteract TGF-β release and glioma cell motility and invasiveness already at low micromolar doses, troglitazone represents a promising drug for adjuvant therapy of glioma and other highly migratory tumor entities. [Mol Cancer Ther 2007;6(6):1745–54]

Introduction

Gliomas are the most common primary tumors in the central nervous system, with glioblastomas as the most malignant entity (1). Despite multimodal therapy regimens, including neurosurgical resection, radiochemotherapy, and polychemotherapy, the prognosis of glioma patients remains poor. Less than 3% of affected patients survive >5 years after diagnosis (2). Rapid proliferation and diffuse brain invasion are histopathologic hallmarks of these tumors and are likely to determine unfavorable prognosis. Among the plethora of molecular-genetic abnormalities identified within cell cycle control mechanisms of malignant glioma cells (1), the transforming growth factor-β (TGF-β) signaling pathway plays a decisive role for tumor growth and cell motility (3) and remarkable efforts were initiated to target the TGF-β pathway for adjuvant glioma therapy (4).

The peroxisome proliferator-activated receptor-γ (PPAR-γ) is a ligand-activated transcription factor that belongs to the superfamily of hormone receptors (5). Major physiologic mechanisms of PPAR-γ include the regulation of adipocyte differentiation and glucose homeostasis. The synthetic thiazolidinediones rosiglitazone, pioglitazone, ciglitazone, and troglitazone were developed as specific PPAR-γ activators. Beyond the established clinical use of thiazolidinediones for oral therapy of type 2 diabetes, recent *in vitro* and *in vivo* studies have shown that thiazolidinediones also play an important role as regulators of inflammation, cell proliferation, and resistance to apoptosis in cancer (6). The antitumor efficacy of thiazolidinediones was explored in several *in vitro* and *in vivo* studies as well as in clinical trials addressing angiosarcomas, breast cancers, prostate cancers, advanced melanomas, and soft tissue sarcomas (7). Analysis of the four thiazolidinediones rosiglitazone, pioglitazone, ciglitazone, and troglitazone shown in this study emphasized their potency to reduce glioma cell growth, whereas troglitazone seems to be more efficient than the remaining thiazolidinediones tested. By applying an *ex vivo* tumor implantation model,

Received 12/11/06; revised 3/27/07; accepted 5/1/07.

Grant support: Nolting Stiftung (University of Cologne; E. Hahnen), the ELAN-Fonds (University of Erlangen-Nuremberg), and the Wilhelm Sander-Stiftung (WSS 2005.089.1; I.Y. Eyüpoglu and I. Blümcke).

The costs of publication of this article were defrayed in part by the payment of page charges. This article must therefore be hereby marked *advertisement* in accordance with 18 U.S.C. Section 1734 solely to indicate this fact.

Requests for reprints: Eric Hahnen, Institute of Human Genetics, University of Cologne, Kerpenerstr. 34, 50931 Cologne, Germany. Phone: 49-221-478-86464; Fax: 49-221-478-86465. E-mail: eric.hahnen@uk-koeln.de

doi:10.1158/1535-7163.MCT-06-0763

micromolar doses of troglitazone diminished glioma progression in an organotypic brain environment. We show that this property is based on the ability of troglitazone to induce cell cycle arrest and to reduce glioma cell migration and brain invasion. Troglitazone-induced inhibition of glioma cell motility occurred in a PPAR-γ–independent manner and is in concordance with its ability to modulate the expression of genes involved in TGF-β signaling. Based on the identification of troglitazone as a potent inhibitor of TGF-β release in glioma cells already at low micromolar doses and the increasing evidence for a prominent role of TGF-β in glioma cell motility, troglitazone and troglitazone derivatives may be considered for adjuvant glioma therapy to counteract TGF-β–mediated brain invasion.

Materials and Methods

Chemicals

Thiazolidinediones were purchased from Alexis Biochemicals. GW9662 and SB431542 were obtained from Sigma-Aldrich. All compounds were dissolved in DMSO and diluted in cell culture medium before experimental use.

Monolayer Culture

SMA-560 mouse glioma cells (8) were kindly provided by D.D. Bigner (Duke University, Durham, NC). The rat glioma cell line F98 and the human glioma cell line U-87 MG were obtained from the American Type Culture Collection. Glioma cells were cultivated as described (9).

Cell Proliferation and Cytotoxicity Assays

Cell proliferation was measured using the 3-(4,5-dimethylthiazol-2-yl)-2,5-diphenyl-tetrazolium-bromide (MTT) assay (10) as described (9) and using the 5-bromo-2′-deoxyuridine labeling and detection kit III (Roche). For the 5-bromo-2′-deoxyuridine assay, 50,000 cells/mL were seeded into 96-well plates (100 μL/well), treated as described for MTT assay (9), and analyzed after 96 h according to the manufacturer's protocol. Lactate dehydrogenase, a cytosolic enzyme that is released from the cell upon loss of plasma membrane integrity, was measured using the CytoTox 96 Assay (Promega) according to the manufacturer's protocol (10,000 cells per well using 96-well plates, 48 h). For all assays, each experiment was repeated eight times ($n = 8$).

Flow Cytometry

Forty thousand cells per milliliter were seeded in 25 cm^2 culture flasks. After incubation with the test compound or solvent only, cells were washed in PBS, fixed in methanol, washed twice in PBS, and incubated with PBS containing 2% FCS and 40 μg/mL RNase A (Roche). Cells were suspended in PBS containing 20 μg/mL propidium iodide (Sigma-Aldrich). The rate of apoptosis and the cell cycle distribution were analyzed by flow cytometry (10,000 counts per sample) using FACSCalibur equipped with Cell Quest software (BD Biosciences). The data were evaluated using Win MDI version 2.8 (TSRI) and Cylchred version 1.0.2 (Cardiff University, Wales, United Kingdom) as described (11, 12). For each experiment, analyses were repeated thrice ($n = 3$).

RNA Isolation and ReverseTranscription-PCR Analysis

RNA isolation was done using the RNeasy Mini Kit (Qiagen). For nonquantitative analyses, reverse transcription was done using oligodeoxythimidylate primers and 1 μg of total RNA by applying the SuperScript First-Strand Synthesis System (Invitrogen). Two microliters of each 20 μL reverse transcription reaction were used for each reverse transcription-PCR (RT-PCR). Mouse, rat, and human *β-actin* and *PPAR-γ* cDNA were amplified using primers that bind to all three orthologues of each gene (*β-actin*-fwd AACGGCTCCGGCATGTGCAA, *β-actin*-rev CTCAAACATGATCTGGGTCATCTT; *PPARγ*-fwd CATGCTTGTGAAGGATGCAAG, *PPARγ*-rev CCCATCATTAAGGAATTCATGTC). PCR conditions were as follows: 5 min initial denaturation (94°C), followed by 36 cycles (94°C for 45 s, 60°C for 45 s, 72°C for 45 s) and final extension (72°C for 7 min). PCR products were visualized on agarose gels by ethidium bromide staining. For quantitative RT-PCR analyses, one-step RT-PCR was preformed using the QuantiTect SYBR Green RT-PCR kit and validated QuantiTect Primer Assays (Qiagen) on an Applied Biosystems 7500 Real-time PCR System. Each 20 μL RT-PCR reaction contained 10 ng total RNA. To ensure that equal amounts of total RNA have been used for each analysis, the exact RNA concentration of each sample was determined by applying the RiboGreen RNA Quantitation Kit (Invitrogen) using a Tecan Safire^2 microplate reader (Tecan). The following QuantiTect primer assays were used: *Tgf-β$_1$*, *Tgf-β$_2$*, *Tgf-β$_3$*, *Tgf-βrI*, *Tgf-βrII*, and *Fkbp1a*. The comparative method of relative quantification ($2^{-\Delta Ct}$) was used to calculate the expression levels of each target gene relative to time- and solvent-matched controls. The RT-PCR specificity was verified by melting curve analysis. Real-time RT-PCR was conducted thrice for each gene and each RNA sample with four technical repetitions ($n = 12$).

Organotypic Entorhino-Hippocampal Slice Cultures

Organotypic entorhino-hippocampal slice cultures (OHSC) were prepared and maintained according to the interface technique (13) as described in detail (9). In brief, 7-day-old Wistar rats were decapitated; the brains were rapidly removed and placed into ice-cold preparation medium. After dissection of the frontal pole of the hemispheres and the cerebellum, the brains were cut in 350-μm-thick horizontal slices using a vibratome (Leica VT 1000S) in preparation medium. Brain slices were transferred onto culture plate insert membranes (Becton Dickinson; 0.4 μm pore diameter) and subsequently into six-well culture dishes containing 1.2 mL OHSC medium (9). The medium was changed 1 day after preparation and every 2nd day thereafter. For the assessment of potential neurotoxicity to rat brain parenchyma, OHSCs were treated either with the test compound or solvent only. The medium, including the test compound or solvent, was changed every 2nd day. Six days after initial treatment, irreversibly damaged cell bodies were visualized by propidium iodide staining as described (14). For each experiment, eight brain slices were used ($n = 8$).

Organotypic Glioma Invasion Model

Transfection of the pEGFP-N1 expression vector (Clontech) into F98 glioma cells was done as described (9, 15). Transfected cells were cultured in selection medium containing 500 μg G418/mL (Sigma-Aldrich). Green fluorescent protein (GFP)–positive F98 glioma cells (5,000) were implanted within a total volume of 0.1 μL medium into the entorhinal cortex 1 day after slice preparation (9, 14). One day after implantation and every following day, glioma growth and invasion were evaluated using a fluorescence microscope as described below. Seven brain slices were used for each experiment ($n = 7$).

Monolayer Wound-Healing and *In vitro* Migration Assay

Cell migration was analyzed using the monolayer wound-healing assay as described (16). Glioma cells were cultured until confluency was achieved. Scratch wounds were added using standard 1,000 μL pipette tips followed by treatment with the test compound or solvent only. The wounds were monitored by phase contrast microscopy. Images were taken at 2-h intervals over the time course of 12 to 24 h and analyzed as described below. Eight images were used for each experiment ($n = 8$). The *in vitro* migration assay was done using a Boyden chamber (QCM-FN Migration Assay, Chemicon). Briefly, 2.5×10^5 F98 glioma cells, pretreated with the test compound/compounds or solvent for 24 h, were transferred into each Boyden chamber. At 24 h after incubation, cells that migrated through the fibronectin-coated chamber membranes (8 μm pore diameter) were quantified according to the manufacturer's protocol. Experiments were repeated thrice ($n = 3$).

Microscopic Evaluation

Morphometric analyses were done using high-power optical fields digitized with a charge coupled device camera (Color View II, Soft Imaging System) equipped with a BX51 microscope (Olympus) using analySIS documentation software (Soft Imaging System). Fluorescence (enhanced GFP)–labeled tumor cells transplanted into OHSCs as well as propidium iodide staining intensities were analyzed by an Olympus IX70 microscope equipped with a tetramethyl rhodamine isothiocyanate (excitation filter 520–550 nm, barrier filter 580 nm) and FITC (excitation filter 450–490 nm, band filter 520–550) narrow band filter and a charge coupled device camera (F-View II; Soft Imaging System).

Immunoblot Analyses

For the analysis of TGF-$\beta_{1\text{-}3}$ expression in cell culture supernatants, F98 glioma cells were cultivated as described. Forty percent to 50% confluent F98 cell cultures were washed with PBS, cultivated in serum-free DMEM medium, and treated with the test compound or solvent only for 48 h. Cell culture supernatants were collected and centrifuged to remove persistent cells, followed by protein concentration using Amicon Ultra-15 centrifugal filter devices (Millipore). After centrifugation (45 min, 4000 × *g*, room temperature), the concentrated retentates (30 μg total protein per lane) were subjected to Western blot analyses using standard protocols (12% SDS-PAGE). Equal loading of each well was confirmed by Ponceau staining. The rabbit polyclonal antibody TGF-β1/2/3 (H-112; Santa Cruz Biotechnology) was added in a dilution of 1:250 to detect all three TGF-β variants. PPAR-γ and β-actin expression levels in rat brain and F98 whole-cell lysates were analyzed using rabbit polyclonal PPAR-γ (1:400, Abcam) and mouse monoclonal β-actin (1:20,000, Sigma-Aldrich) antibodies. Peroxidase-conjugated goat anti-rabbit IgG (1:10,000, Pierce) and goat anti-mouse IgG (1:10,000, Jackson ImmoResearch) were used as secondary antibodies. Detection of signals was carried out using the Super Signal West Pico chemiluminescence reagent (Pierce).

TGF-β_1 Quantification (ELISA)

To quantify TGF-β_1 protein levels in glioma cell culture supernatants, ELISA assays were done according to the manufacturer's protocols (Mouse/Rat/Porcine/Canine Quantikine TGF-β1, Human Quantikine TGF-β1 ELISA Kit, R&D Systems). Briefly, a monoclonal antibody specific for the mature TGF-β_1 ligand has been precoated onto the bottom of 96-well plates. Standards, controls, and samples are transferred into the wells and any TGF-β_1 present is bound by the immobilized antibody. Subsequently, an enzyme-linked polyclonal antibody against TGF-β_1 was added to the wells to sandwich the immobilized TGF-β_1. A substrate solution is added to the wells and color develops in proportion to the amount of TGF-β_1 bound in the initial step. The absorbance was measured using a Tecan Safire^2 microplate reader at an absorbance of 450 nm (reference wavelength 540 nm). Each experiment was repeated thrice ($n = 3$).

Data Analysis

Concentration-effect curves were analyzed by nonlinear regression analysis (GraphPad Software 4.03) as described (9), by applying a four-variable logistic equation containing the variables top plateau, bottom plateau, inflection point (IC_{50}), and curve slope. Drug concentrations inducing a 50% and 90% reduction of cell growth/TGF-β_1 release, respectively, were read from the best-fit curves. For statistical analysis, single comparisons were analyzed by unpaired *t* tests, whereas multiple comparisons among the data sets were done by two-way ANOVA (GraphPad). Three levels of statistical significance were discriminated (*, $P < 0.05$; **, $P < 0.01$; ***, $P < 0.001$).

Results

The Antiproliferative Effects of Troglitazone Do Not Correlate with PPAR-γ Expression

Concentration-dependent inhibition of glioma cell growth by PPAR-γ agonists was investigated using cell lines derived from mouse (SMA-560), rat (F98), and human (U-87 MG). As shown by MTT assay, all compounds inhibited glioma cell growth in a concentration-dependent manner. The reduction of cell growth occurred with steep curve slopes and consequently there was a narrow range of effective concentrations producing a 10% to 90% inhibition

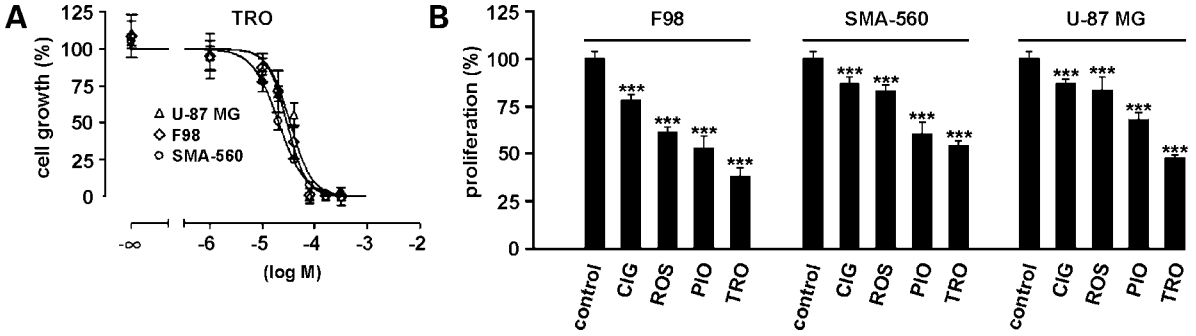

Figure 1. Thiazolidinediones reduce glioma cell proliferation in a dose-dependent manner. **A,** concentration-dependent inhibition of glioma cell growth (MTT assay) by troglitazone (*TRO*) in the indicated cell lines. *Points,* mean percentage relative to time- and solvent-matched controls; *bars,* SD. For troglitazone and the remaining drugs (not shown), IC_{50} and IC_{90} concentrations, defined as concentrations shown to inhibit tumor cell viability by 50% or 90%, respectively, were determined by nonlinear regression analysis as follows: ciglitazone (F98, 44 and 102 μmol/L; SMA-560, 37 and 91 μmol/L; U-87 MG, 36 and 85 μmol/L), rosiglitazone (F98, 32 and 120 μmol/L; SMA-560, 46 and 115 μmol/L; U-87 MG, 63 and 159 μmol/L), pioglitazone (F98, 46 and 145 μmol/L; SMA-560, 51 and 148 μmol/L; U-87 MG, 85 and 158 μmol/L). Troglitazone (F98, 30 and 76 μmol/L; SMA-560, 20 and 74 μmol/L; U-87 MG, 34 and 98 μmol/L). **B,** using 40 μmol/L doses in a 5-bromo-2′-deoxyuridine assay, all test compounds significantly ($P < 0.001$, *t* test) reduced glioma cell proliferation compared with the respective control; irrespective of the cell line, applied troglitazone displayed a significantly higher effect compared with ciglitazone (*CIG*) and rosiglitazone (*ROS*; $P < 0.001$, *t* test). Differences in effect between troglitazone and pioglitazone (*PIO*) reached levels of significance ($P < 0.01$, *t* test) using U-87 MG cells. In F98 and SMA-560 cells, the stronger effect of troglitazone compared with pioglitazone was confirmed using 80 μmol/L doses (data not shown). *Columns,* mean percentage relative to the time- and solvent-matched controls; *bars,* SD.

(Fig. 1A). Irrespective of the drug and cell line tested, the IC_{50} was found at doses ranging from 20 to 85 μmol/L (variables characterizing the cell growth inhibition are given in Fig. 1 legend). With IC_{50} doses of 20 μmol/L (SMA-560), 30 μmol/L (F98), and 34 μmol/L (U-87 MG), troglitazone seemed to be more potent than the remaining thiazolidinediones tested. The reduction of glioma cell proliferation was confirmed by measuring 5-bromo-2′-deoxyuridine uptake. Using 40 μmol/L doses, all compounds significantly reduced glioma cell proliferation, whereas troglitazone again had a higher efficacy compared with the remaining drugs (Fig. 1B). The cell lines did not essentially differ in their dose-dependent response to each drug ($P > 0.05$, two-way ANOVA). This finding is particularly interesting because the PPAR-γ receptor is expressed in SMA-560 and U-87 MG, but only barely detectable in F98 glioma cells (Fig. 2A and B). Treatment of F98 cells with IC_{50} (30 μmol/L) or IC_{90} (76 μmol/L) doses of troglitazone did not induce PPAR-γ expression (Fig. 2C). In all, these data suggest that the antiproliferative effects of troglitazone do not correlate with PPAR-γ expression.

Troglitazone Causes G_1 Arrest but Does Not Induce F98 Glioma Cell Death

Subsequent analyses focused on troglitazone due to its superior efficacy compared with the remaining test drugs. Consistent with previous findings using other cancer cell types (17–21), repeated flow cytometric analyses of F98 glioma cells after exposure to IC_{90} concentrations of troglitazone for 48 h revealed a significant accumulation of glioma cells in the G_1 phase (control, 34.5 ± 2.2%;

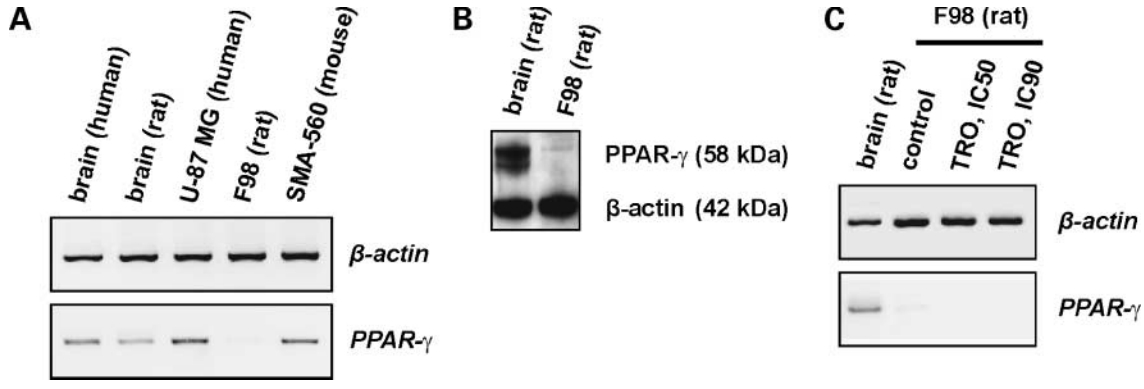

Figure 2. PPAR-γ is barely detectable in F98 glioma cells. **A,** as shown by RT-PCR analysis, *PPAR-γ* is abundantly expressed in rat and human brain as well as in SMA-560 and U-87 MG, but barely detectable rat F98 glioma cells. **B,** Western blot analysis confirmed a very weak PPAR-γ expression in rat F98 glioma cells compared with rat brain. Two PPAR-γ isoforms (PPAR-γ1, PPAR-γ2) were detected in rat brain, which derived from alternative splicing (49). In F98 cells, only a faint PPAR-γ1 signal was detected. **C,** *PPAR-γ* expression is not induced after treatment of F98 cells with IC_{50} or IC_{90} doses of troglitazone for 48 h as shown by RT-PCR.

troglitazone IC_{90}, 46.6 ± 3.5%; $P < 0.05$, t test) and reduction of cells in the S phase (control, 44.2 ± 7.2%; troglitazone IC_{90}, 32.0 ± 4.0%; $P < 0.05$, t test), confirming that troglitazone blocks events critical for G_1-S progression. The share of cells in the G_2 phase was not significantly altered compared with time- and solvent-matched controls (control, 17.2 ± 6.0%; troglitazone IC_{90}, 16.3 ± 2.2%; $P > 0.05$, t test). The proportion of apoptotic cells in the sub-G_1 phase was also not significantly elevated (control, 4.2 ± 1.7%; troglitazone IC_{90}, 5.1 ± 2.3%, $P > 0.05$, t test). Consistently, exposure of F98 cells to troglitazone IC_{90} concentrations did not increase lactate dehydrogenase release ($P > 0.05$, t test, data not shown), indicating that troglitazone acts antiproliferative rather than proapoptotic in F98 cells at the doses used.

Troglitazone Blocks Glioma Progression *Ex Vivo* but Does not Reduce Existing Tumor Size

We used rat organotypic hippocampal brain slice cultures (OHSC) to monitor glioma cell proliferation and brain invasion in the organotypic brain environment (9). Initially, potential neurotoxic effects of troglitazone were evaluated *ex vivo* using the rat OHSC model. Increased propidium iodide uptake, which indicates irreversible cell damage, was not observed after treatment with IC_{90} (76 μmol/L) or 2× IC_{90} (152 μmol/L) concentrations, indicating that troglitazone is not neurotoxic to highly vulnerable rat brain parenchyma at concentrations shown to effectively diminish glioma cell proliferation *in vitro* (data not shown). To evaluate the propensity of troglitazone to reduce glioma progression in an organotypic brain environment, enhanced GFP–labeled F98 glioma cells were implanted into the entorhinal cortex of OHSCs (Fig. 3A). The tumor infiltration area was quantified each day after implantation up to 6 days by fluorescence microscopy. A continuous increase of the bulk tumor mass was observed in solvent-matched control experiments at all time periods. Six days after implantation, the tumor infiltration area increased ~11-fold compared with the initial tumor size at day 1 after implantation (Fig. 3B and C). In contrast, the tumor infiltration size remained stable over the period of 6 days after treatment with IC_{90} doses, indicating that troglitazone effectively impeded tumor progression *ex vivo* (Fig. 3B

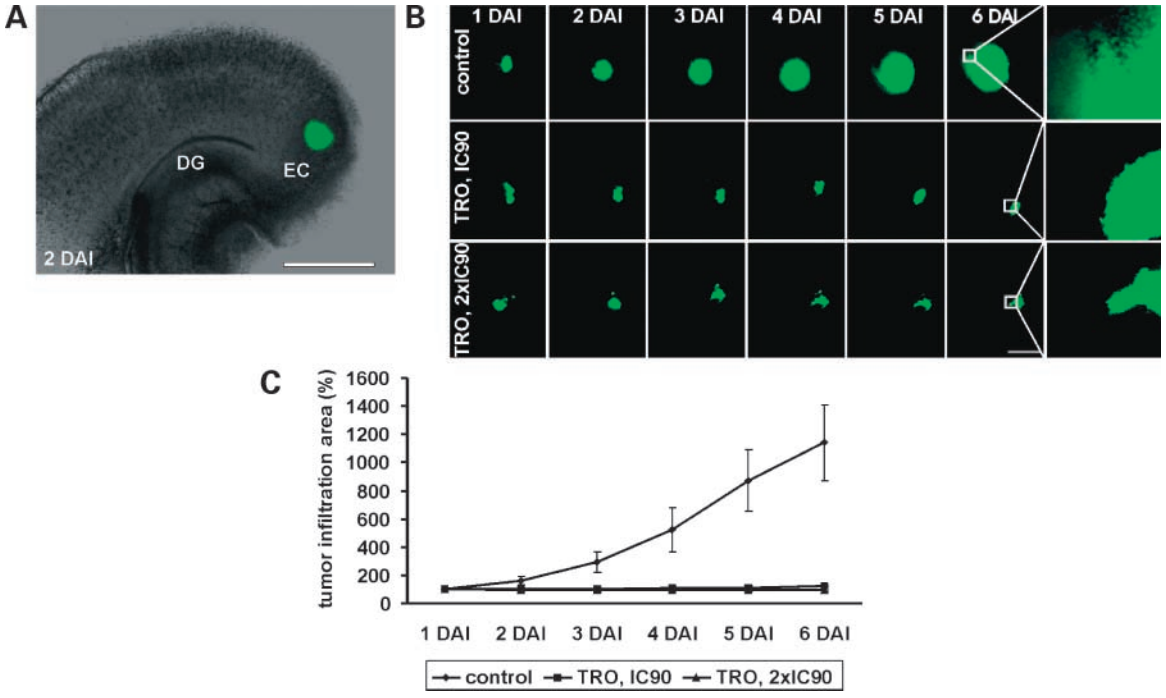

Figure 3. Troglitazone inhibits glioma progression in an organotypic glioma transplantation model. **A,** organotypic glioma invasion model. Five thousand enhanced GFP–positive F98 rat glioma cells were transplanted into the entorhinal cortex 1 d after organotypic rat brain slice culture preparation. Fluorescence microscopic image superimposed onto a translucent image of the same slice culture. *DAI,* days after implantation; *DG,* dentate gyrus; *EC,* entorhinal cortex. Bar, 200 μm. **B,** after transplantation of enhanced GFP–positive F98 glioma cells into the entorhinal cortex of the brain slice cultures, tumor progression was monitored by fluorescent microscopy over the time course of 6 d. Results of three representative experiments. Bar, 200 μm. *Right column,* magnification of the indicated border area between bulk tumor mass and rat brain tissue. In controls, F98 glioma cells have diffusely migrated into the adjacent brain parenchyma, whereas a sharp tumor border was observed after troglitazone treatment. **C,** quantification of the tumor infiltration area at days 1 to 6 after transplantation derived from seven independent experiments in each of the three groups. For each experiment, the tumor infiltration area at 1 d after implantation was defined as 100%. *Points,* mean percentage; *bars,* SD. A continuous increase of the bulk tumor masses was observed in solvent-matched controls whereas IC_{90} and 2× IC_{90} doses of troglitazone effectively blocked tumor progression. At 6 d after implantation, the tumor infiltration area increased to 1,139 ± 384% in solvent-matched controls but remained unchanged after troglitazone treatment (IC_{90} 126 ± 13%; 2× IC_{90} 94 ± 8%). Differences in tumor progression between controls and troglitazone-treated samples reached levels of significance starting at 2 d after implantation ($P < 0.01$, t test).

and C). Increased, nontoxic doses of troglitazone (2× IC_{90}), diminished tumor progression in a similar manner as observed after treatment with IC_{90} concentrations (Fig. 3B and C). Interestingly, even 2× IC_{90} doses of troglitazone were not capable to significantly reduce initial tumor infiltration area ($P > 0.05$, t test), which is consistent with the absence of apoptotic tumor cell death after troglitazone treatment (see above). This finding indicates that troglitazone is not able to reduce existing tumor masses, but effectively inhibits tumor progression in an organotypic environment.

Troglitazone PPAR-γ Independently Inhibits Glioma Cell Migration *In Vitro* and *Ex Vivo*

Using the rat organotypic tumor invasion model, we have shown that enhanced GFP–labeled F98 glioma cells migrate into the adjacent brain parenchyma, visible as a diffuse corona surrounding the bulk tumor mass (9). Diffuse infiltration of F98 cells into the brain parenchyma was observed in solvent-matched controls, but not after treatment with IC_{90} and 2× IC_{90} doses of troglitazone (Fig. 3B). Thus, we hypothesized that the lack of tumor progression and brain invasion observed after troglitazone treatment was accompanied by a reduction of glioma cell migration. By applying a monolayer wound-healing assay, we showed that the F98 glioma cell locomotion was substantially altered by troglitazone (Fig. 4A and B). After mechanical injury, bordering glioma cells show a lamellar protusion and migration toward the center of the wound, resulting in a progressive reduction of the wound area (Fig. 4A). In control experiments, the wound area was reduced by 30 ± 5% at 12 h and by 53 ± 6% at 22 h after injury, respectively, whereas the reduction of the wound area was diminished in a dose-dependent manner after troglitazone treatment (Fig. 4A and B). To confirm this finding, glioma cell migration was further analyzed by using a Boyden chamber assay. Compared with the migratory activity of solvent-treated controls, troglitazone dose-dependently decreased F98 glioma cell migration by 83.3 ± 2.3% (IC_{50}) and 90.8 ± 2.1% (IC_{90}), respectively. The migratory activity of solvent-treated F98 cells and the antimigratory effects of troglitazone were not impaired by the irreversible and selective PPAR-γ inhibitor GW9662 (22), indicating that the antimigratory properties of troglitazone were not PPAR-γ mediated (Fig. 4C).

Transcriptional Down-regulation of *Tgf-β* and its Receptors *Tgf-βrI* and *Tgf-βrII* by Troglitazone

TGF-β signaling has shown to be crucially implicated in glioma cell migration and brain invasion. Exogenously added TGF-β_1 and TGF-β_2 were found to elicit a strong stimulation of migration and invasiveness in a variety of glioma cells *in vitro* (23–26), whereas small interfering RNA–mediated *Tgf-β₁* and *Tgf-β₂* gene silencing has shown to counteract glioma cell motility and invasiveness (27). Consistently, selective inhibition of TGF-β signaling by SB431542, a small-molecule inhibitor of the type I TGF-β receptor kinase activity (28), reduced F98 migration by 73.9 ± 1.9% similar to troglitazone (Fig. 4C). Based on this finding, we hypothesized that troglitazone is able to counteract TGF-β–mediated glioma cell migration and

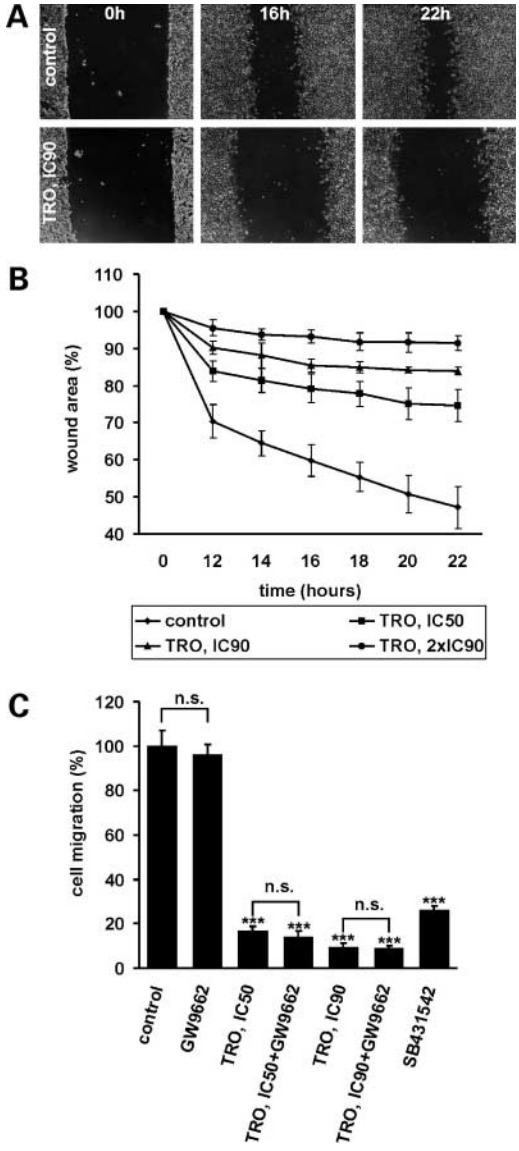

Figure 4. Troglitazone inhibits glioma cell migration. **A,** analysis of F98 glioma cell migration by monolayer wound-healing assay. Phase contrast micrographs of F98 glioma cell cultures treated with IC_{90} doses of troglitazone or solvent only at various times after monolayer wounding. **B,** quantification of F98 glioma cell migration by monolayer wound-healing assay. For each experiment, wound healing was monitored over a time course of 12 to 22 h (2 h intervals). *Points,* mean relative to the initial wound area defined as 100%; *bars,* SD. At all time points and all concentrations analyzed, troglitazone significantly inhibited glioma cell migration compared with solvent-matched controls ($P < 0.001$, t test). Dose-dependent differences reached levels of significance ($P < 0.05$, t test). **C,** quantification of F98 glioma cell migration by Boyden chamber assay. Treatment of F98 glioma cells with IC_{50} and IC_{90} doses of troglitazone significantly reduced migration by 83.3 ± 2.3% and 90.8 ± 2.1%, respectively, compared with solvent-matched controls (100 ± 6.9%, $P < 0.001$, t test). PPAR-γ inhibition by GW9662 (20 μmol/L) neither affected the migratory activity of solvent-matched F98 cells (96.2 ± 4.6 %) nor the antimigratory effects of troglitazone (troglitazone IC_{50} and GW9662 86.3 ± 3.1; troglitazone IC_{90} and GW9662 91.3 ± 1.2%). Inhibition of TGF-β signaling by SB431542 (10 μmol/L) decreased the F98 cell migration by 73.9 ± 1.9%.

brain invasion. Three variants of TGF-β (TGF-β_{1-3}) are encoded by three homologous genes. Real-time PCR analysis revealed a dose-dependent down-regulation of *Tgf-β_{1-3}* and their receptors (*Tgf-βrI, Tgf-βrII*) after troglitazone treatment, whereas the *FK506-binding protein 1A* (*Fkbp1a*) gene expression, which encoded the protein that inhibits TGF-β receptor I activity (29), remained unchanged (Fig. 5). To analyze the levels of released TGF-β_{1-3}, supernatants of F98 glioma cell cultures were subjected to immunoblotting. Using a polyclonal antibody directed against all three TGF-β isoforms, TGF-β–specific signals were abundant in solvent-matched controls, but not after troglitazone treatment (IC_{90}), giving evidence that troglitazone decreased the TGF-β release to very low levels (Fig. 6A). A comparative real-time PCR analysis of basal *Tgf-β_{1-3}* expression levels in nontreated F98 cells identified >2^6-fold higher expression levels of *Tgf-β_1* compared with *Tgf-β_3* and *Tgf-β_2*, thus identifying *Tgf-β_1* as the predominant *Tgf-β* isoform (data not shown).

Troglitazone Reduces TGF-β_1 Release at Low Micromolar Doses

Extracellular TGF-β_1 and TGF-β_2 concentrations of 2 to 5 ng/mL cell culture medium have shown to elevate the migratory activity of glioma cells (24, 25). We did an absolute TGF-β_1 quantification to assess whether F98 glioma cells release TGF-β_1 at relevant doses. Promigratory concentrations of 5.92 ng/mL (±0.10 ng/mL) cell culture medium were observed in solvent-matched controls, suggesting that F98 cells promote migration by an autocrine signaling pathway. In contrast, troglitazone decreased TGF-β_1 protein levels by 94.93 ± 0.22% using IC_{50} and almost completely using IC_{90} doses, respectively, to 0.30 ng (±0.01 ng) and 0.01 ng/mL (±0.00 ng/mL). An extended, dose-dependent analysis revealed that already 7.41 μmol/L doses of troglitazone reduced TGF-β_1 release by 50%. A very similar reduction was observed in SMA-560 and U87-MG glioma cells. Both cell lines released TGF-β_1 at relevant doses (SMA-560, 2.37 ± 0.11 ng/mL; U87-MG, 2.30 ± 0.02 ng/mL), whereas 8.32 and 8.51 μmol/L doses of troglitazone, respectively, reduced TGF-β_1 levels by 50%, thus identifying troglitazone as a potent inhibitor of TGF-β_1 release at low micromolar concentrations (Fig. 6B). Using 10 μmol/L concentrations, the remaining test compounds also reduced TGF-β_1 release in all cell lines tested, but significantly less efficient than troglitazone (Fig. 6C).

Discussion

The thiazolidinediones rosiglitazone, pioglitazone, ciglitazone, and troglitazone decreased glioma cell proliferation in a dose-dependent manner, whereas troglitazone showed a superior potency in all cell lines tested (Fig. 1A and B). The effects of troglitazone on the cell cycle distribution have intensively been studied in various cancer cell lines (17–21). We confirmed that troglitazone causes a G_1 arrest, which has shown to be associated with altered expression levels of genes critically involved in the G_1-S cell cycle progression (17–21, 30). For example, troglitazone has shown to increase the expression of the *DNA damage inducible gene 45* (*Gadd45*) as well as the cyclin-dependent kinase inhibitors *$p21^{CIP1/WAF1}$* and *$p27^{KIP}$* and down-regulates the expression of the cyclin-dependent kinases *Cdk2, Cdk4*, and *Cdk6* and the DNA polymerase δ auxiliary protein (*Pcna*), a nuclear protein whose appearance correlates with the proliferative state of the cell. By quantitative real-time PCR analysis, we confirmed that troglitazone (IC_{50}, IC_{90}) significantly reduced the expression of *Pcna, Cdk2, Cdk4*, and *Cdk6*, and increased the *Gadd45* expression in F98 glioma cells in a dose-dependent manner (data not shown), suggesting that the troglitazone-induced G_1 arrest identified in F98 glioma and other neoplastic cells share common mechanisms. However, the effects of troglitazone on the F98 glioma cell transcriptome are by far not restricted to the genes described. A preliminary microarray analysis (Affymetrix REA230A) revealed that the expression of 4.0% (643 of 15,923) of all transcripts was at least 2-fold increased, whereas the expression of 7.9% (1,258 of 15,923) of all transcripts was

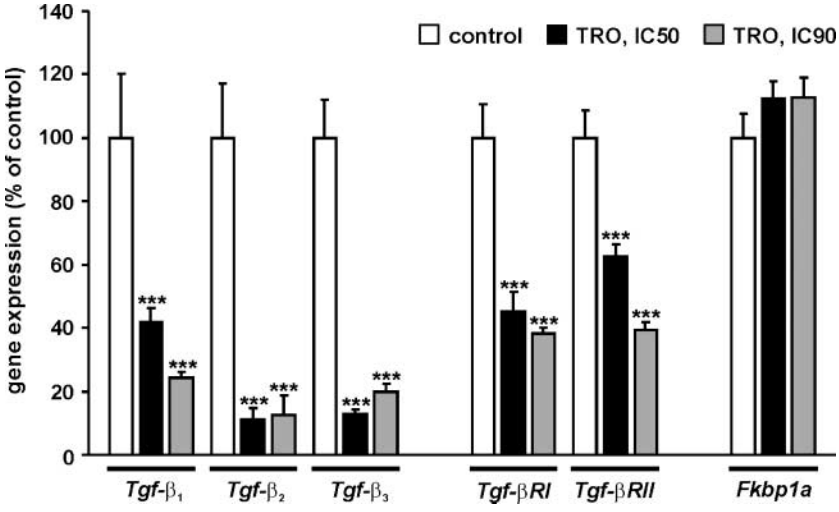

Figure 5. Troglitazone modulates the expression of genes involved in TGF-β signaling. Gene expression levels were examined by real-time PCR analyses of F98 glioma cells after treatment with IC_{50} and IC_{90} doses of troglitazone, respectively, for 48 h. *Columns,* real-time PCR data, mean percentage relative to the expression levels in time- and solvent-matched controls; *bars,* SD (***, $P < 0.001$, *t* test).

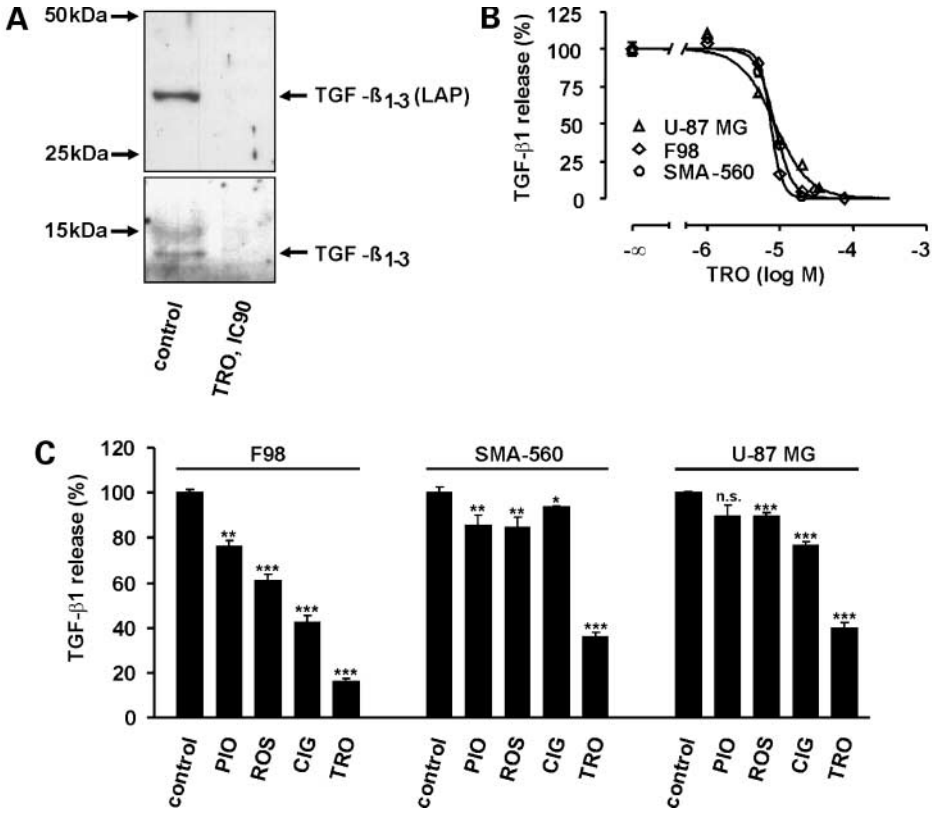

Figure 6. Troglitazone reduces TGF-β release at low micromolar doses. **A**, TGF-β–releasing cells secrete two molecular forms of the *Tgf-β1-3* gene products, which resemble cleavage products of the pre-pro TGF-β proteins (50). These isoforms are the COOH-terminal mature and biologically active TGF-β peptides with molecular weights of ~12 kDa and the NH_2-terminal peptides known as latency associated proteins (*LAP*). Using a polyclonal antibody directed against all three TGF-β isoforms, TGF-β signals (mature TGF-β_{1-3}, TGF-β latency associated protein) were detected in solvent-matched controls, but not after troglitazone treatment. Equal loading of each well was confirmed by Ponceau staining. **B**, quantification of TGF-β_1 release in F98, SMA-560, and U87-MG glioma cell culture supernatants after troglitazone treatment. Troglitazone concentrations shown to inhibit TGF-β1 release by 10%, 50%, or 90%, respectively, were determined by nonlinear regression analysis: F98, 5.01, 7.41, and 10.96 μmol/L; SMA-560, 4.57, 8.32, and 15.48 μmol/L; U-87 MG, 2.51, 8.51, and 25.11 μmol/L. **C**, using 10 μmol/L doses, all test compounds (pioglitazone, rosiglitazone, ciglitazone, and troglitazone) reduced TGF-β_1 levels released by F98, SMA-560, and U87-MG glioma cells compared with the respective controls. Irrespective of the glioma cell line applied, troglitazone displayed a significantly higher effect compared with the remaining test compounds ($P < 0.001$, *t* test).

decreased by 50% or more after troglitazone treatment (IC_{90}, 48 h), indicating that troglitazone has extensive pleitropic effects on the glioma cell transcriptome.

The primary mechanism(s) by which troglitazone modulates the expression of genes involved in glioma cell proliferation and cell cycle distribution remain elusive. The PPAR family of ligand-activated transcription factors consists of three subtypes (PPAR-γ, PPAR-α, and PPAR-δ), which form heterodimers with the nuclear retinoid X receptor and then bind to PPAR response elements in the regulatory regions of target genes. Although pioglitazone and rosiglitazone activate both PPAR-γ and PPAR-α, respectively, troglitazone has shown to be PPAR-γ selective (31). Several lines of evidence support that the inhibitory effects of thiazolidinediones on tumor cell proliferation are not PPAR-γ mediated. As confirmed in our study, the sensitivity of cancer cells to thiazolidinedione-mediated growth inhibition does not correlate with the level of PPAR-γ expression (Figs. 1 and 2) and there exists a three orders of magnitude discrepancy between the concentration required to produce antitumor effects and that to improve insulin resistance via PPAR-γ activation (32). Using PPAR-γ–positive and PPAR-γ–deficient mouse embryonic stem cells, it has been shown that troglitazone inhibited the growth of tumors formed by injection of PPAR-γ +/+ and PPAR-γ −/− embryonic stem cells to the same extent, indicating that PPAR-γ is not essential for the antiproliferative effects of troglitazone (33). Moreover, troglitazone derivatives that are unable to activate PPAR-γ suppress cancer cell proliferation similar to troglitazone, giving further evidence that the antiproliferative effects of troglitazone are PPAR-γ independent (32).

Using the rat organotypic glioma invasion model, we show that micromolar doses of troglitazone are capable to block glioma progression (Fig. 3). This intriguing antiglioma property of troglitazone seems to be only partially based on its antiproliferative effects, which have been suggested to be moderate (32). In subsequent analyses, we identified troglitazone as a potent inhibitor of glioma cell migration and diffuse brain invasion, which occurs in a

PPAR-γ–independent manner (Figs. 3 and 4). The antimigratory effects of troglitazone could be mimicked by inhibition of TGF-β signaling, which has shown to be intimately involved in glioma cell migration, suggesting both mechanisms to be interlinked (Fig. 4C). Several studies using surgically resected glioma tissues revealed an intriguing correlation between tumor grade and the expression of TGF-$\beta_{1\text{-}3}$ and their receptors I and II. High-grade gliomas express high levels of TGF-βRI, TGF-βRII, and TGF-$\beta_{1\text{-}3}$, whereas the expression levels of these molecules have shown to be weak in low-grade gliomas and normal brain tissue (34–36). The inverse correlation between TGF-$\beta_{1\text{-}3}$, TGF-βRI, and TGF-βRII expression and patient's survival support its pivotal role in malignant glioma progression. The role of TGF-β as molecular target for glioma therapy has been facilitated by numerous studies demonstrating that TGF-β levels determine glioma cell motility. Exogenously added TGF-β_1 and TGF-β_2 elicit a strong stimulation of migration in a variety of glioma cells (23–26), whereas *Tgf-*β_1 and *Tgf-*β_2 gene silencing has shown to reduce glioma cell motility and invasiveness (27). We identified troglitazone to significantly down-regulate the expression of *Tgf-*$\beta_{1\text{-}3}$ and their receptors (*Tgf-βrI, Tgf-βrII*), whereas expression of Fkbp1a, a protein that inhibits TGF-βRI activity (29), remained unchanged (Fig. 5). Using a polyclonal antibody directed against all three TGF-β isoforms, we show that troglitazone substantially decreased TGF-β release (Fig. 6A). An absolute quantification of TGF-β_1 protein levels revealed that rat F98, mouse SMA-560, and human U87-MG glioma cells release TGF-β_1 at relevant doses, suggesting that glioma cells promote migration by an autocrine signaling pathway. A dose-dependent analysis indicated that troglitazone significantly inhibits TGF-β_1 release already at low micromolar doses in all three glioma cell lines applied, with a narrow range of concentrations producing a 10% to 90% inhibition (Fig. 6B). In all, these results are in line with the propensity of troglitazone to counteract TGF-β–mediated glioma cell motility and invasiveness into brain parenchyma (Figs. 3 and 4).

Several studies are consistent with our finding that troglitazone counteracts TGF-β signaling. For example, TGF-β has shown to increase the expression of the matrix metalloproteinases MMP-2 and MMP-9, thus promoting glioma cell migration (3, 37), whereas troglitazone has shown to decrease MMP-2 and MMP-9 protein levels (38). TGF-β has shown to induce the expression of the caspase-8 inhibitor FLICE inhibitory protein, which plays a critical role as an endogenous modulator of apoptosis (39, 40). In contrast, troglitazone has shown to cause a pronounced reduction of FLICE inhibitory protein levels in glioma cells, thus sentisizing glioma cells to tumor necrosis factor–related apoptosis-inducing ligand–induced apoptosis (41). Moreover, troglitazone significantly counteracts hepatocellular carcinoma, thyroid cancer, and prostate cancer progression in xenograft mouse models (18, 42, 43). Especially the present data concerning prostate cancer and glioma treatment seem to share similarities. Very similar to glioma cells, TGF-β_1 promotes the motility of prostate cancer cells (44), whereas elevated TGF-β expression is associated with poor clinical outcome (45). A phase II clinical study in prostate cancer patients revealed a prolonged stabilization of prostate-specific antigen and long periods of stable disease in patients treated with troglitazone (46). In reference to these findings, one might speculate that numerous effects of troglitazone described thus far are due to its ability to counteract TGF-β signaling.

Because TGF-β antagonism is considered as a therapeutic strategy, including the development of antisense regimens, inhibition of pro–TGF-β processing, scavenging of TGF-β by the TGF-β–binding protein decorin, and blocking of TGF-β receptor I kinase activity (4), our results suggest troglitazone as a candidate drug for adjuvant glioma therapy. Pharmacokinetic studies in healthy individuals revealed that, after p.o. application of 400 mg of troglitazone, serum levels of 5.42 mg/L (12.3 μmol/L) can be achieved (47). At these doses, troglitazone displayed only marginal effects on glioma cell proliferation (Fig. 1A), but effectively inhibited TGF-β_1 release *in vitro* (Fig. 6B and C). With regard to the pharmacokinetic data, one might speculate that only antimigratory but not antiproliferative doses of troglitazone are clinically achievable. It has not been established whether troglitazone penetrates the blood-brain barrier in humans; however, rat studies provide evidence that troglitazone is actively incorporated by the bidirectional transporter Oatp14 (Slco1c1) expressed in brain capillary endothelial cells, which is likely to provide troglitazone homeostasis (48). We show that the antimigratory effects of troglitazone are PPAR-γ independent (Fig. 4C). Thus, the yet unknown protein/proteins mediating the troglitazone-induced inhibition of brain invasion and/or glioma proliferation remain to be identified and may represent future targets for structure-relationship studies. Moreover, already established antiproliferative and PPAR-γ–inactive troglitazone derivatives (32) may retain their propensity to counteract TGF-β–dependent glioma cell migration and might be further developed to minimize potential PPAR-γ–mediated side effects in glioma patients. Because local invasion of neoplastic cells into the surrounding brain is perhaps the most important aspect on the biology of gliomas that precludes successful treatment, troglitazone and its derivatives may be considered for the adjuvant therapy of glioma and other highly migratory tumor entities.

References

1. DeAngelis LM. Brain tumors. N Engl J Med 2001;344:114 – 23.
2. Ohgaki H, Kleihues P. Epidemiology and etiology of gliomas. Acta Neuropathol (Berl) 2005;109:93 – 108.
3. Wick W, Platten M, Weller M. Glioma cell invasion: regulation of metalloproteinase activity by TGF-β. J Neurooncol 2001;53:177 – 85.
4. Wick W, Naumann U, Weller M. Transforming growth factor-β: a molecular target for the future therapy of glioblastoma. Curr Pharm Des 2006;12:341 – 9.
5. Kliewer SA, Xu HE, Lambert MH, Willson TM. Peroxisome proliferator-activated receptors: from genes to physiology. Recent Prog Horm Res 2001;56:239 – 63.
6. Hafner C, Reichle A, Vogt T. New indications for established drugs: combined tumor-stroma-targeted cancer therapy with PPARγ agonists, COX-2 inhibitors, mTOR antagonists and metronomic chemotherapy. Curr Cancer Drug Targets 2005;5:393 – 419.

7. Grommes C, Landreth GE, Heneka MT. Antineoplastic effects of peroxisome proliferator-activated receptor γ agonists. Lancet Oncol 2004; 5:419 – 29.

8. Sampson JH, Ashley DM, Archer GE, et al. Characterization of a spontaneous murine astrocytoma and abrogation of its tumorigenicity by cytokine secretion. Neurosurgery 1997;41:1365 – 72; discussion 72 – 3.

9. Eyupoglu IY, Hahnen E, Buslei R, et al. Suberoylanilide hydroxamic acid (SAHA) has potent anti-glioma properties *in vitro, ex vivo* and *in vivo*. J Neurochem 2005;93:992 – 9.

10. Mosmann T. Rapid colorimetric assay for cellular growth and survival: application to proliferation and cytotoxicity assays. J Immunol Methods 1983;65:55 – 63.

11. Ormerod MG, Payne AW, Watson JV. Improved program for the analysis of DNA histograms. Cytometry 1987;8:637 – 41.

12. Watson JV. Proof without prejudice revisited: immunofluorescence histogram analysis using cumulative frequency subtraction plus ratio analysis of means. Cytometry 2001;43:55 – 68.

13. Stoppini L, Buchs PA, Muller D. A simple method for organotypic cultures of nervous tissue. J Neurosci Methods 1991;37:173 – 82.

14. Eyupoglu IY, Hahnen E, Trankle C, et al. Experimental therapy of malignant gliomas using the inhibitor of histone deacetylase MS-275. Mol Cancer Ther 2006;5:1248 – 55.

15. Eyupoglu IY, Hahnen E, Heckel A, et al. Malignant glioma-induced neuronal cell death in an organotypic glioma invasion model. Technical note. J Neurosurg 2005;102:738 – 44.

16. Valster A, Tran NL, Nakada M, Berens ME, Chan AY, Symons M. Cell migration and invasion assays. Methods 2005;37:208 – 15.

17. Motomura W, Okumura T, Takahashi N, Obara T, Kohgo Y. Activation of peroxisome proliferator-activated receptor γ by troglitazone inhibits cell growth through the increase of p27KiP1 in human. Pancreatic carcinoma cells. Cancer Res 2000;60:5558 – 64.

18. Yu J, Qiao L, Zimmermann L, et al. Troglitazone inhibits tumor growth in hepatocellular carcinoma *in vitro* and *in vivo*. Hepatology 2006;43: 134 – 43.

19. Yoshizawa K, Cioca DP, Kawa S, Tanaka E, Kiyosawa K. Peroxisome proliferator-activated receptor γ ligand troglitazone induces cell cycle arrest and apoptosis of hepatocellular carcinoma cell lines. Cancer 2002; 95:2243 – 51.

20. Yin F, Wakino S, Liu Z, et al. Troglitazone inhibits growth of MCF-7 breast carcinoma cells by targeting G_1 cell cycle regulators. Biochem Biophys Res Commun 2001;286:916 – 22.

21. Guan YF, Zhang YH, Breyer RM, Davis L, Breyer MD. Expression of peroxisome proliferator-activated receptor γ (PPARγ) in human transitional bladder cancer and its role in inducing cell death. Neoplasia 1999;1: 330 – 9.

22. Leesnitzer LM, Parks DJ, Bledsoe RK, et al. Functional consequences of cysteine modification in the ligand binding sites of peroxisome proliferator activated receptors by GW9662. Biochemistry 2002;41: 6640 – 50.

23. Merzak A, McCrea S, Koocheckpour S, Pilkington GJ. Control of human glioma cell growth, migration and invasion *in vitro* by transforming growth factor β 1. Br J Cancer 1994;70:199 – 203.

24. Platten M, Wick W, Wild-Bode C, Aulwurm S, Dichgans J, Weller M. Transforming growth factors β(1) (TGF-β(1)) and TGF-β(2) promote glioma cell migration via Up-regulation of α(V)β([3]) integrin expression. Biochem Biophys Res Commun 2000;268:607 – 11.

25. Wick W, Grimmel C, Wild-Bode C, Platten M, Arpin M, Weller M. Ezrin-dependent promotion of glioma cell clonogenicity, motility, and invasion mediated by BCL-2 and transforming growth factor-β2. J Neurosci 2001;21:3360 – 8.

26. Uhl M, Aulwurm S, Wischhusen J, et al. SD-208, a novel transforming growth factor β receptor I kinase inhibitor, inhibits growth and invasiveness and enhances immunogenicity of murine and human glioma cells *in vitro* and *in vivo*. Cancer Res 2004;64:7954 – 61.

27. Friese MA, Wischhusen J, Wick W, et al. RNA interference targeting transforming growth factor-β enhances NKG2D-mediated antiglioma immune response, inhibits glioma cell migration and invasiveness, and abrogates tumorigenicity *in vivo*. Cancer Res 2004;64:7596 – 603.

28. Hjelmeland MD, Hjelmeland AB, Sathornsumetee S, et al. SB-431542, a small molecule transforming growth factor-β-receptor antagonist, inhibits human glioma cell line proliferation and motility. Mol Cancer Ther 2004;3:737 – 45.

29. Stockwell BR, Schreiber SL. TGF-β-signaling with small molecule FKBP12 antagonists that bind myristoylated FKBP12-TGF-β type I receptor fusion proteins. Chem Biol 1998;5:385 – 95.

30. Yin F, Bruemmer D, Blaschke F, Hsueh WA, Law RE, Herle AJ. Signaling pathways involved in induction of GADD45 gene expression and apoptosis by troglitazone in human MCF-7 breast carcinoma cells. Oncogene 2004;23:4614 – 23.

31. Sakamoto J, Kimura H, Moriyama S, et al. Activation of human peroxisome proliferator-activated receptor (PPAR) subtypes by pioglitazone. Biochem Biophys Res Commun 2000;278:704 – 11.

32. Weng JR, Chen CY, Pinzone JJ, Ringel MD, Chen CS. Beyond peroxisome proliferator-activated receptor γ signaling: the multi-facets of the antitumor effect of thiazolidinediones. Endocr Relat Cancer 2006;13: 401 – 13.

33. Palakurthi SS, Aktas H, Grubissich LM, Mortensen RM, Halperin JA. Anticancer effects of thiazolidinediones are independent of peroxisome proliferator-activated receptor γ and mediated by inhibition of translation initiation. Cancer Res 2001;61:6213 – 8.

34. Kjellman C, Olofsson SP, Hansson O, et al. Expression of TGF-β isoforms, TGF-β receptors, and SMAD molecules at different stages of human glioma. Int J Cancer 2000;89:251 – 8.

35. Kawataki T, Naganuma H, Sasaki A, Yoshikawa H, Tasaka K, Nukui H. Correlation of thrombospondin-1 and transforming growth factor-β expression with malignancy of glioma. Neuropathology 2000;20:161 – 9.

36. Yamada N, Kato M, Yamashita H, et al. Enhanced expression of transforming growth factor-β and its type-I and type-II receptors in human glioblastoma. Int J Cancer 1995;62:386 – 92.

37. Rooprai HK, Rucklidge GJ, Panou C, Pilkington GJ. The effects of exogenous growth factors on matrix metalloproteinase secretion by human brain tumour cells. Br J Cancer 2000;82:52 – 5.

38. Liu J, Lu H, Huang R, et al. Peroxisome proliferator activated receptor-γ ligands induced cell growth inhibition and its influence on matrix metalloproteinase activity in human myeloid leukemia cells. Cancer Chemother Pharmacol 2005;56:400 – 8.

39. Maedler K, Fontana A, Ris F, et al. FLIP switches Fas-mediated glucose signaling in human pancreatic β cells from apoptosis to cell replication. Proc Natl Acad Sci U S A 2002;99:8236 – 41.

40. Schlapbach R, Spanaus KS, Malipiero U, et al. TGF-β induces the expression of the FLICE-inhibitory protein and inhibits Fas-mediated apoptosis of microglia. Eur J Immunol 2000;30:3680 – 8.

41. Schultze K, Bock B, Eckert A, et al. Troglitazone sensitizes tumor cells to TRAIL-induced apoptosis via down-regulation of FLIP and Survivin. Apoptosis 2006;11:1503 – 12.

42. Ohta K, Endo T, Haraguchi K, Hershman JM, Onaya T. Ligands for peroxisome proliferator-activated receptor γ inhibit growth and induce apoptosis of human papillary thyroid carcinoma cells. J Clin Endocrinol Metab 2001;86:2170 – 7.

43. Kubota T, Koshizuka K, Williamson EA, et al. Ligand for peroxisome proliferator-activated receptor γ (troglitazone) has potent antitumor effect against human prostate cancer both *in vitro* and *in vivo*. Cancer Res 1998;58:3344 – 52.

44. Morton DM, Barrack ER. Modulation of transforming growth factor β1 effects on prostate cancer cell proliferation by growth factors and extracellular matrix. Cancer Res 1995;55:2596 – 602.

45. Bello-DeOcampo D, Tindall DJ. TGF-βI/Smad signaling in prostate cancer. Curr Drug Targets 2003;4:197 – 207.

46. Mueller E, Smith M, Sarraf P, et al. Effects of ligand activation of peroxisome proliferator-activated receptor γ in human prostate cancer. Proc Natl Acad Sci U S A 2000;97:10990 – 5.

47. Loi CM, Young M, Randinitis E, Vassos A, Koup JR. Clinical pharmacokinetics of troglitazone. Clin Pharmacokinet 1999;37:91 – 104.

48. Sugiyama D, Kusuhara H, Taniguchi H, et al. Functional characterization of rat brain-specific organic anion transporter (Oatp14) at the blood-brain barrier: high affinity transporter for thyroxine. J Biol Chem 2003;278:43489 – 95.

49. Bogazzi F, Ultimieri F, Raggi F, et al. Abnormal expression of PPAR γ isoforms in the subcutaneous adipose tissue of patients with Cushing's disease. Clin Endocrinol (Oxf) 2007;66:7 – 12.

50. Dubois CM, Laprise MH, Blanchette F, Gentry LE, Leduc R. Processing of transforming growth factor β1 precursor by human furin convertase. J Biol Chem 1995;270:10618 – 24.